UDC 629.5.052.3+621.396.67.012.12

UNIFORM RECTANGULAR ARRAY RADAR OPTIMIZATION FOR EFFICIENT AND ACCURATE ESTIMATION OF TARGET PARAMETERS

Vadim V. Romanuke

Polish Naval Academy, Gdynia, Poland

Background. If the intensity of moving targets within a surveyed area is low, some sensors of the uniform rectangular array (URA) radar can be (symmetrically) turned off. However, this does not guarantee detection of any target because sometimes the threshold detection, by which the main parameters of the target are estimated, fails.

Objective. In order to improve detection of ground-surface targets, the goal is to find an optimal number of URA radar sensors along with improving the stage of threshold detection. The criterion is to determine such a minimum of these sensors at which the main parameters of the target are accurately estimated. In addition, the threshold detection is to be modified so that a number of detection fails would be lesser.

Methods. To achieve the said goal, the URA radar is simulated to detect a single target. The simulation is configured and carried out by using MATLAB® R2021b Phased Array System Toolbox™ functions based on a model of the monostatic radar.

Results. There is a set of quasioptimal URA sizes included minimally-sized and maximally-sized URAs. The best decision is to use, at the first stage, the minimally-sized URA (by turning off the maximal number of vertical and horizontal sensors). If the detection fails, then the maximally-sized URA radar is tried. If the detection fails again, the next minimally-sized URA is tried, in which one horizontal sensor is additionally turned on. Additional horizontal sensors must be enabled while the detection fails but the number of vertical sensors should not be greater by about a third of their minimal number.

Conclusions. An optimal number of URA radar sensors is in either the minimally-sized URA (or close to it) or maximally-sized URA (or close to it). The URA size is regulated by (symmetrically) turning off vertical and horizontal sensors. The threshold detection stage is modified so that the threshold is gradually decreased while the detection fails. This allows increasing a number of detected targets on average, which is equivalent to increasing the probability of detection.

Keywords: *phased array radar; uniform rectangular array; surveyed area; target; detection threshold; accuracy.*

1. Phased array radar surveillance system

To observe and control presence of one or multiple objects within a nearby area, phased array radars are used [1], [2]. In a ground-surface surveillance system using a uniform rectangular array (URA) to observe and control, the beam of radio waves is electronically steered to point in different directions (at different azimuth angles) without turning the antenna elements (URA sensors) [3], [4]. This is done owing to the phase shifters [1], [3], [4]. The phase shifters delay the radio waves progressively so that each sensor emits its wavefront in a specific order. This causes the resulting plane wave to be directed at an angle to the URA. The computer quickly alters the phase shifters to steer the beam to a new direction, which usually is in the neighbourhood of the previous direction [2], [5], [6]. The URA radar thus scans an area, where the scanning range of azimuth angles can be up to 90° and wider.

Unlike the application of URAs for other tasks, the URA surveillance system does not synthesize a specific beam pattern for ensuring signal selectivity by direction [7], [8]. However, the beam pattern mainlobe for a URA surveillance system must be symmetric and sufficiently narrow at any scanning direction [9], [10]. Moreover, to maintain low interference, the beam sidelobes must be cancelled at both the azimuth and elevation angles (Fig. 1).

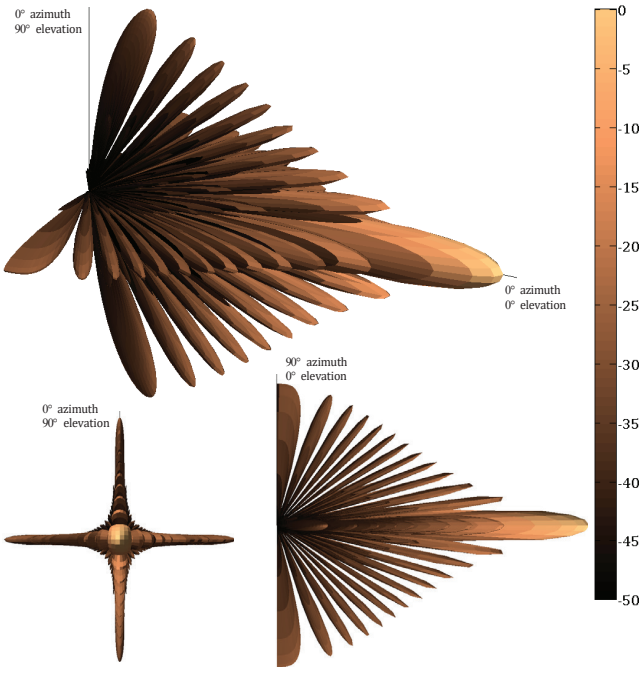

Fig. 1. A 20×25 **URA response pattern (the colorbar is normalized power in dB)**

Although the ground-surface URA radar does not observe or control presence at (positive) elevation angles, the power emitted at elevations should be as low as possible [1], [5], [11], [12]. This is why URA vertical sensors are used in such radars. For instance, the number of vertical sensors of the URA in Fig. 1 is less than the number of horizontal sensors, but still those 20 sensors ensure small losses of power at elevations and additionally form a narrow "pencil" beam mainlobe [7], [8], [13]. A radar of URA with only 5 vertical sensors would be quite inefficient (Fig. 2).

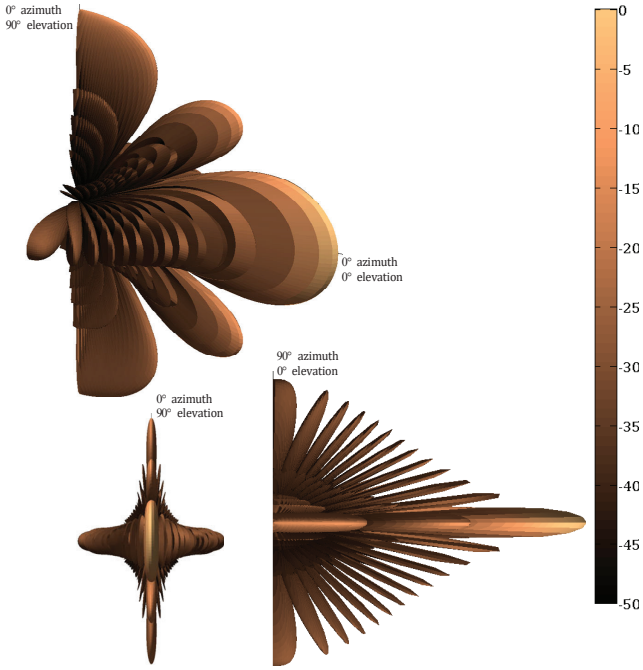

Fig. 2. A 5×25 URA response pattern, where the ineffectiveness of the 5×25 URA radar is seen (compared to that in Fig. 1) due to much power is emitted at elevations and the beam mainlobe is not sufficiently narrow at the side elevation view (although it is quite narrow at the pattern view from "above" being similar to that in Fig. 1)

Various tasks of radar surveillance systems require different configuration of URA. It depends also on the intensity of moving targets within a surveyed area [10], [14], [15]. If the intensity is low, then, for instance, some sensors of the URA radar can be (symmetrically) turned off [16], [17]. Otherwise, all the URA sensors emit. However, this does not guarantee detection of any target. Sometimes the threshold detection [18], [19], by which the main parameters of the target are estimated, fails. Therefore, the problem can be considered in two parts. First, an optimal number of URA sensors, which should be turned on, is to be determined. Second, the routine for the detection threshold is to be improved.

2. Goal and tasks to achieve it

In order to improve detection of ground-surface targets, the goal is to find an optimal number of URA radar sensors along with improving the stage of threshold detection. The criterion is to determine such a minimum of these sensors at which the main parameters of the target are accurately estimated [20]. In addition, the threshold detection is to be modified so that a number of detection fails would be lesser. To achieve the said goal, the URA radar is to be simulated by using MATLAB® R2021b Phased Array System Toolbox™ (PAST) functions. First, the simulation parameters and set-up are to be described. Along with that, an algorithm of a softer adjustment of the detection threshold will be stated. Next, the functioning of the URA radar is simulated for a set of randomly generated targets, where the URA size is changed through a set of possible URA sizes. Changing the URA size is meant by turning on or off some sensors [4], [8], [21], [22]. The simulation will be carried out for both the known threshold detection approach and the softer adjustment approach. The results obtained from the simulation are expected to allow making decisions on how to optimize the URA radar for efficient and accurate estimation of target parameters [20], [23]. All limitations, tradeoffs, and controversies of the optimization will be discussed.

3. Simulation parameters and set-up

It is supposed that a URA is used in a monostatic radar to periodically scan a predefined surveillance area [1], [24], [25]. The purpose is to detect a target in this region and estimate its main parameters — distance d to the target (in terms of radar systems, it is called the range), azimuth angle α, and velocity v. The target is only sought in the azimuth dimension, and the radar is required to search from $45°$ to $-45°$ in azimuth.

The radar design meets the following typical specifications [2], [5], [26], [27]: detection probability is $p_{\text{det}}=0.9$, probability of false alarm is $p_{\text{FA}}=10^{-6}$, maximum unambiguous range is $r_{\max}=5000$ (in meters), target radar cross section is 1 m^2, the number of pulses to integrate is 10.

A URA radar is created by using the PAST environment and functions. Its parameters are as follows [28], [29]:

1) the operating frequency $f_{\text{oper}}=10$ GHz;

2) the sampling frequency $f_{\text{sampl}}=5995849.16$ Hz;

3) the pulse repetition frequency (f_{PR}) is presumed to be a $1/200$ part of the sampling frequency, so it is $f_{\text{PR}}=29979.2458$ Hz.

The array consists of w horizontal and h vertical elements. The antenna elements are configured so that they only emit forward [3], [7], [30], [31]. Then, using radar equations, the array gain, signal-to-noise ratio, and the peak power are calculated. Thus, the peak power of the transmitter is set.

The scanning schedule of the URA has the revisit time which is less than 1 second. This means that the radar should revisit the same azimuth angle within 1 second. The required number of scans is determined by the beamwidth of the array response [7], [8], [32], [33]. The 3 dB beamwidth θ (in degrees) is estimated by using the array gain. Then the scan step δ_{scan} is selected so that $\delta_{\text{scan}} < \theta$. This is done for allowing for some beam overlap in space. In addition, the scan step must not be greater than $6°$ in order to hold a sufficiently dense scan grid. Thus,

$$\delta_{\text{scan}} = \min\left\{6, \rho(\theta)\right\} \tag{1}$$

by function $\rho(\theta)$ returning the integer part of number θ (e. g., see [34], [35]).

The scan grid $G_{\text{scan}} = \left\{\vartheta_i\right\}_{i=1}^{K}$ is formed to be uniform and symmetric with a step of δ_{scan} calculated by (1). It starts with

$$\vartheta_1 = 45 - \frac{90 - \rho\left(\dfrac{90}{\delta_{\text{scan}}}\right)\cdot\delta_{\text{scan}}}{2} = \rho\left(\frac{90}{\delta_{\text{scan}}}\right)\cdot\frac{\delta_{\text{scan}}}{2} \tag{2}$$

and goes down with a step of $-\delta_{\text{scan}}$ until $\vartheta_K \geqslant -45°$:

$$\vartheta_{i+1} = \vartheta_i - \delta_{\text{scan}} \text{ for } i = \overline{1, K-1}. \tag{3}$$

The total number of pulses is $10\cdot K$, so the revisit time is

$$t_{\text{rev}} = \frac{10\cdot K}{f_{\text{PR}}} = \frac{10\cdot K}{29979.2458} \approx$$
$$\approx 0.0003335640952\cdot K. \tag{4}$$

As the URA is grown in size, the revisit time increases due to the scan grid becomes denser (and thus number K increases). However, even for relatively huge URAs (of 100×100 size and bigger) revisit time (4) is far less than 1 second.

The target is assumed to be at $0°$ elevation and it is a non-fluctuating object. The pulse returning from the target is to be simulated. The total simulation time corresponds to one pass through the surveillance region. Because the reflected signals are received by the URA, a beamformer pointing to the steering direction is used to obtain the combined signal. Thus, the URA receiving beamformer is created in the PAST environment. Then a propagation channel for the target is defined.

A pulse is generated, emitted, radiated toward the target, and reflected off the target. This is repeated for $10\cdot K$ pulses. Then the received signal is processed by passing it through a matched filter and integrating all pulses for each scan angle.

To estimate target parameters $\left\{d, \alpha, v\right\}$, a threshold detection on the scan map is fulfilled. The detection threshold γ is firstly calculated based on the number of pulses to be integrated and noise power at the receiver. Then, however, the threshold is increased by the matched filter processing gain.

At the stage of threshold detection, the pulse integration (this is another pulse integration step; not to be confused with the pulse integration at the matched filtering stage) is fulfilled by compensating for signal power loss due to range by applying time varying gains to the received signal [18], [19]. The result of the pulse integration is a matrix

$$\mathbf{Q} = \left[q_{ji}\right]_{200\times K}$$

whose elements are very small (roughly between 10^{-20} and 10^{-6}). Then inequality

$$q_{ji}^2 > \gamma \tag{5}$$

is analyzed to estimate the range and angle of the target. Those indices j and i for which inequality (5) holds (denote them by j^* and i^*) point to the estimated range (distance to the target) and azimuth angle, respectively. This is done by mapping index j^* on a grid of ranges

$$G_{\text{range}} = \left\{r_j\right\}_{j=1}^{200} = \left\{25\cdot(j-1)\right\}_{j=1}^{200},$$

whereas index i^* is mapped on the scan grid G_{scan}. Thus, the estimated range d^* and azimuth angle α^* are determined. If inequality (5) does not hold, indices j^* and i^* are not found, and then the detection is counted as a fail.

The radial velocity (in meters per second) v^* of the target is calculated based on the Doppler shift [1], [10], where matched filtering pulses, indices j^*, i^*, and pulse repetition frequency f_{PR} are used. First, the Doppler spectrum from the received signal is calculated. Second, its peak points to the respective velocity estimation. However, if the peak is impossible to find, the detection is counted as a fail.

The location of a target is given as a pair of its coordinates

$$\{x, y\} \text{ by } x > 0 \text{ and } y \in \mathbb{R}. \tag{6}$$

The distance to the target is

$$d = \sqrt{x^2 + y^2} \tag{7}$$

and its azimuth angle is

$$\alpha = \frac{180}{\pi} \cdot \arctan\left(\frac{y}{x}\right). \tag{8}$$

During the simulation, coordinates (6) are randomly generated as

$$x = \rho\left(4950\xi + 50\right) \tag{9}$$

and

$$y = \rho\left(4950\zeta_1 + 50\right), \tag{10}$$

where ξ is a value of a random variable uniformly distributed on interval $(0;1)$ and ζ_1 is a value of a random variable distributed normally with zero mean and unit variance [35]. If coordinates (9) and (10) are such that $d > 4975$ or $\alpha > 44°$, their generations by (9) and (10) are repeated until $d \leqslant 4975$ and $\alpha \leqslant 44°$.

The velocity of a target is given in two coordinates:

$$\{v_x, v_y\} \text{ by } v_x \in \mathbb{R} \text{ and } v_y \in \mathbb{R}. \tag{11}$$

Velocity coordinates (11) are randomly generated as

$$v_x = \rho\left(100\zeta_2\right) \tag{12}$$

and

$$v_y = \rho\left(100\zeta_3\right), \tag{13}$$

where ζ_2 and ζ_3 are values of independent random variables distributed normally with zero mean and unit variance. The radial velocity (in meters per second) of the target is calculated as

$$v = -\frac{xv_x + yv_y}{d}. \tag{14}$$

Let the minimal size of URA be 20×25 (Fig. 1) and its maximal size be 35×35 (Fig. 3). These are the marginal sizes, each of which still allows detecting a target correctly but does not guarantee satisfactory results or null fails. The factual size of the URA is 35×35, where a URA of any other size below 35×35 is obtained by turning off the respective number of sensors. Obviously, the turned-off sensors are expected to be in some symmetry with respect to the URA geometry, but peculiarities of this question are not considered here. It is presumed that the symmetry of the sensors to be turned off is calculated and implemented automatically by a special computer routine.

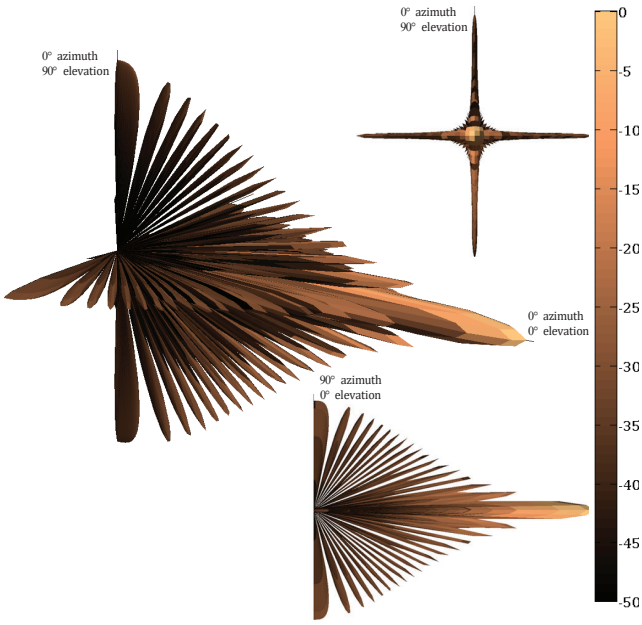

Fig. 3. A 35×35 URA response pattern, which seemingly has a far narrower "pencil" beam mainlobe compared to that in Fig. 1; the sidelobes are further sliced (similarly at the side elevation view and the pattern view from "above"), but it does not always help in accurately estimating the target parameters

For every new target generated by equations (9), (10), (12), (13), the URA size $h \times w$ is changed from 20×25 to 35×35 by the only condition of that $h \leqslant w$. The step of the changing is 1. For obtaining statistically stable results, it is sufficient to simulate 500 random targets.

4. Detection threshold and URA optimization

The detection straightforwardly fails if inequality (5) does not hold. Meanwhile, both sides of this inequality are very small numbers, so the threshold might be corrected even by an insignificant amount at which inequality (5) would turned to be true. So, while

$$q_{ji}^2 \leqslant \gamma \tag{15}$$

the threshold is updated so that it would fit inequality (5):

$$\gamma^{(\text{obs})} = \gamma, \ \gamma = \left(\gamma^{(\text{obs})}\right)^{1.0001}, \tag{16}$$

whereupon inequality (5) is checked again. If inequality (5) is false and $\gamma < 10^{-50}$, the threshold updating is

cancelled and thus the detection is counted as a fail.

For example, if the target has parameters

$$x = 2000,\ y = 1000,\ v_x = 30,\ v_y = 20, \qquad (17)$$

then a 20×25 URA radar using known threshold detection approach with the hard decision by inequality (5) fails to determine the range and azimuth angle (Fig. 4). Here $\gamma = 7.8527 \cdot 10^{-13}$, but if the threshold

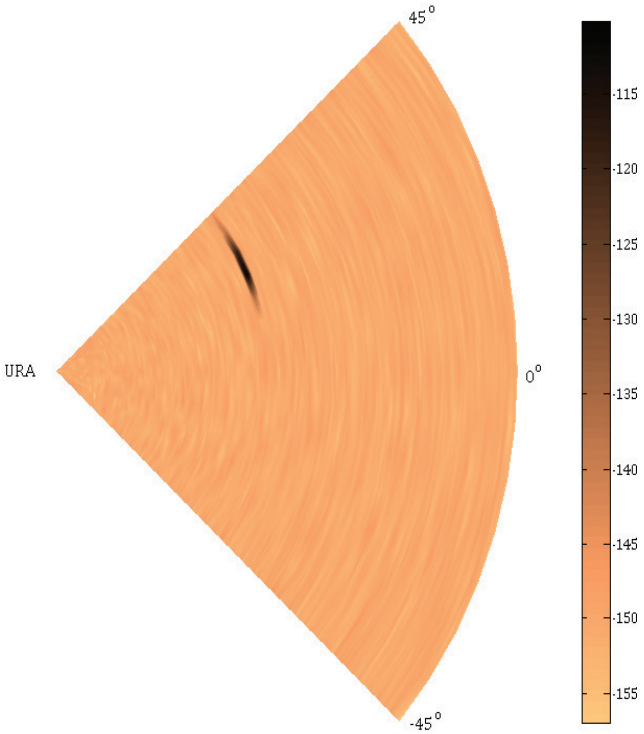

Fig. 4. The scan map from a 20×25 URA radar failing at detection of the target with parameters (17); although the target can be seen (as a blurred arch) in the map, the known threshold detection approach with the hard decision by inequality (5) fails to determine the range and azimuth angle

is adjusted softer, by using (15) and (16), then it is successively updated for 1925 times and inequality (5) becomes true at $\gamma = 2.1162 \cdot 10^{-15}$. This results in a successful detection of the target: whereas the real parameters of the target are

$$d = 2236.068,\ \alpha = 26.5651,\ v = -35.7771, \qquad (18)$$

its estimated parameters

$$d^* = 2225,\ \alpha^* = 30,\ v^* = -35.1076 \qquad (19)$$

are pretty close to (18). Indeed, by using relative differences (in percentage terms)

$$\Delta_d = 100 \cdot \frac{|d^* - d|}{d}, \qquad (20)$$

$$\Delta_\alpha = 100 \cdot \frac{|\alpha^* - \alpha|}{90} = \frac{|\alpha^* - \alpha|}{0.9}, \qquad (21)$$

$$\Delta_v = 100 \cdot \left| \frac{v^* - v}{v} \right| \qquad (22)$$

for the comparison, the real and estimated parameters of the target differ in almost acceptable percentage amounts:

$$\Delta_d = 0.49498,\ \Delta_\alpha = 3.8166,\ \Delta_v = 1.8712. \qquad (23)$$

The exception here may be made for the angle because the inaccuracy in more than $2°$ (with respect to the scanning range of $90°$), which is 2.2222 %, appears to be quite tangible (Fig. 5).

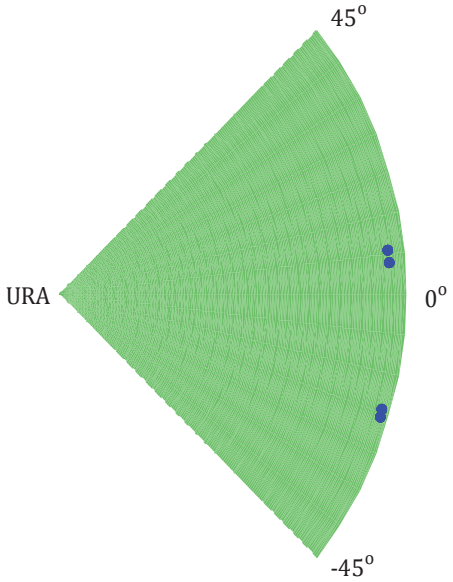

Fig. 5. A demonstration of that the difference in $2°$ azimuth angle (two points above $0°$) is indeed distinguishable; the difference in less than $1.25°$ (which is $\Delta_\alpha = 1.3889$ %) azimuth angle (two points below $0°$) is almost insignificant

Having simulated 500 random targets with (9), (10), (12), (13), only one of 500 targets has not been detected (Fig. 6) by using the softer adjustment of the detection threshold. The target has parameters

$$x = 3805,\ y = -2260,\ v_x = -184,\ v_y = 129.$$

By the known threshold detection approach (the hard decision), the URA radar has detected 405 targets. A comparison of the two approaches is presented in Table 1, where relative difference maximum

$$m_\Delta = \max\{\Delta_d, \Delta_\alpha, \Delta_v\} \qquad (24)$$

is used to show the advantage of the softer adjustment.

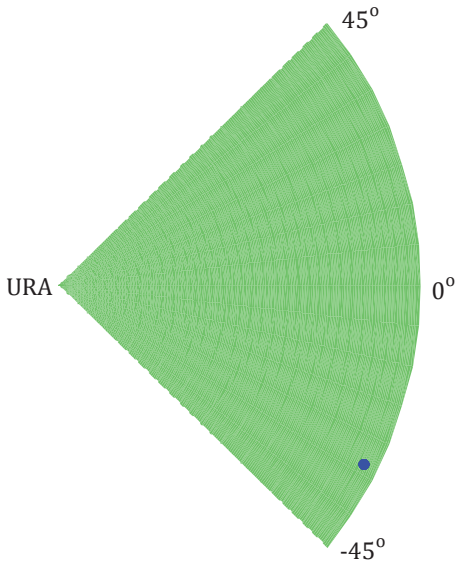

Fig. 6. The single target (out of those 500 ones) which has not been detected by using the softer adjustment of the detection threshold

Table 1. Comparison of the detection threshold softer adjustment to the known threshold detection approach (hard decision)

	Number of instances (targets)	
	Softer adjustment by (15), (16)	Hard decision by (5)
Detection fails	95	1
$m_\Delta < 5$	365	440
$m_\Delta < 4$	358	428
$m_\Delta < 3$	349	404
$m_\Delta < 2$	315	335
$m_\Delta < 1.5$	268	270
$m_\Delta < 1.25$	227	228
$m_\Delta < 1$	169	169

First, the 94 detections failed by the known threshold detection approach and successfully fulfilled by the softer adjustment approach are not considered. Denote by σ the sum of relative difference sums

$$\Delta_\Sigma = \Delta_d + \Delta_\alpha + \Delta_v \qquad (25)$$

for those 405 targets detected by the known threshold detection approach. Similarly to this, denote by σ_{soft} the sum of relative difference sums (25) for those 405 targets detected by the softer adjustment approach. Although the relative difference between the sums calculated as

$$100 \cdot \frac{\sigma - \sigma_{\text{soft}}}{\sigma} \qquad (26)$$

is not that big (it is just 0.7451 %), it nonetheless confirms the advantage of the softer adjustment. Relative difference (26) for the sums taken only for cases when $m_\Delta > 2$ (there are 90 such cases) appears to be little as well: it is 0.8781 %. However, the difference is 0.9405 % for 40 cases when $m_\Delta > 5$, it is 0.9844 % for 25 cases when $m_\Delta > 10$, and it is 1.0173 % for 19 cases when $m_\Delta > 20$ (it is a hardly acceptable detection accuracy). Hence, the detection inaccuracy by the known threshold detection approach grows worse. Relative difference (26) for the sums taken only for 12 cases when $m_\Delta > 100$ (quite unacceptable detection result) is 7.4276 %, so it appears to be significant.

Now the 94 detections are analysed. Their statistics is shown in Table 2 with considering sums (25). It is worth noting that there are no targets detected so accurately that $m_\Delta < 1$. Besides, 19 targets are detected so inaccurately that the detections are unacceptable. The most inaccurate target detection has produced parameter estimations

$$d^* = 4725,\ \alpha^* = 24,\ v^* = -28.0861, \qquad (27)$$

whereas the target had parameters

$$d = 1435.2773,\ \alpha = -39.09,\ v = 9.4086. \qquad (28)$$

Thus,

$$\Delta_d = 229.2047,\ \Delta_\alpha = 70.1,\ \Delta_v = 398.5141 \qquad (29)$$

in this case. The case with (27) — (29) is the worst among all those 499 detections.

Table 2. Statistics for the 94 detections by the detection threshold softer adjustment

	Number of instances (targets)	Minimal Δ_Σ	Average Δ_Σ	Maximal Δ_Σ
$m_\Delta < 5$	75	2.4205	4.3897	7.75218
$m_\Delta < 4$	70	2.4205	4.29538	7.75218
$m_\Delta < 3$	55	2.4205	3.9227	5.6839
$m_\Delta < 2$	20	2.4205	3.16259	4.62358
$m_\Delta < 1.5$	2	2.71836	3.2014	3.6844
$m_\Delta < 1.25$	1	2.71836	2.71836	2.71836
$m_\Delta > 5$	19	9.463278	189.1398	697.8187
$m_\Delta > 7.5$	19	9.463278	189.1398	697.8187
$m_\Delta > 10$	17	89.23369	210.0937	697.8187
$m_\Delta > 15$	17	89.23369	210.0937	697.8187
$m_\Delta > 20$	17	89.23369	210.0937	697.8187
$m_\Delta > 50$	17	89.23369	210.0937	697.8187
$m_\Delta > 100$	5	182.9279	381.7094	697.8187

The answer to the question of why unacceptably inaccurate detections happen remains unclear. Thus, a visualization of all those 500 targets, where hard threshold (HT) and soft threshold (ST) approaches are compared, cannot help in seeing any pattern (Fig. 7). The same-accuracy detections seem randomly scattered.

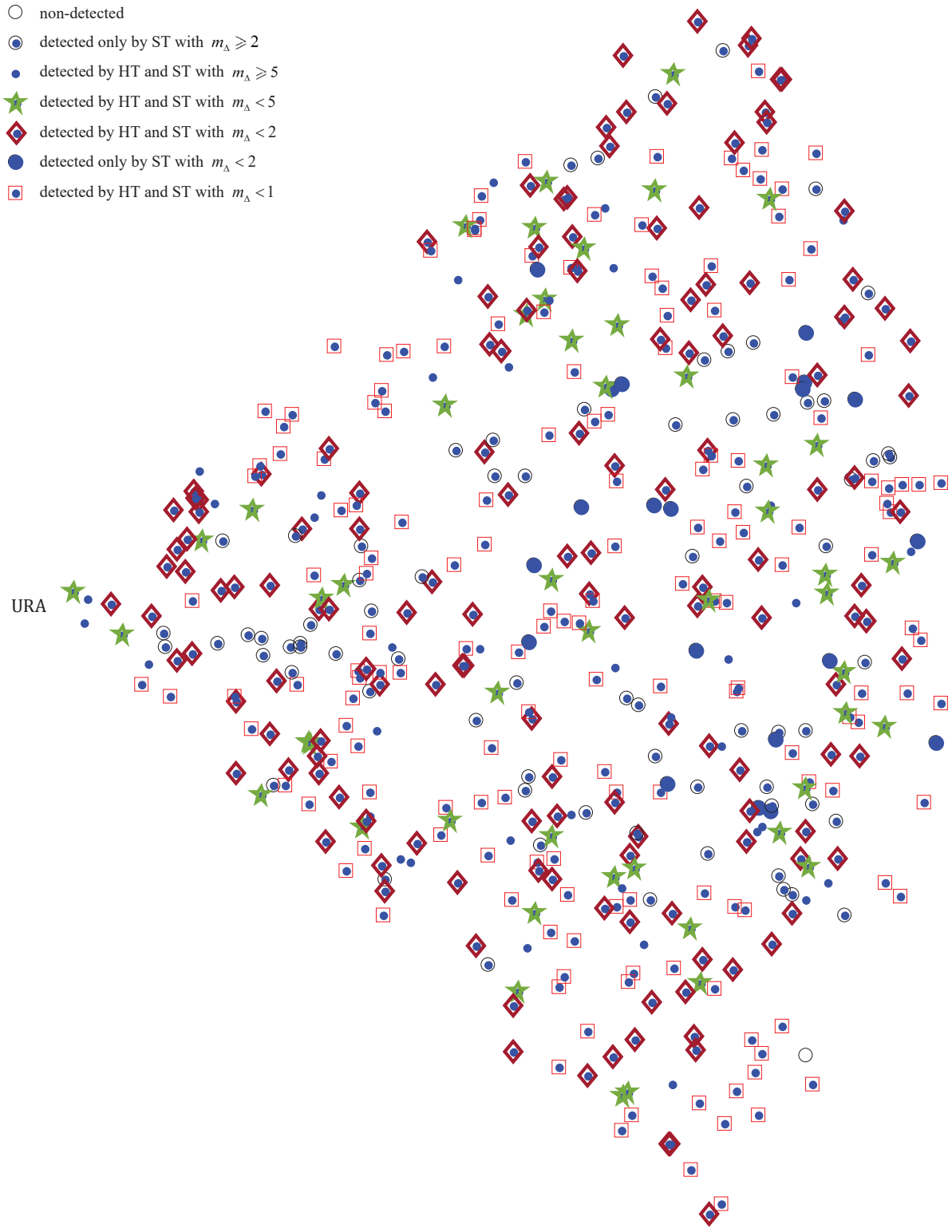

Fig. 7. The scatter of the 500 simulated targets, among which 405 targets have been detected by HT and ST radars, and 94 targets have been detected by only ST radar

Another important question is at which URA size those 499 targets have been detected. Those w horizontal and h vertical URA sensors, at which the detection accuracy has been the best, are marked in Fig. 8 (smaller squares represent the HT radar, and bigger squares represent the ST radar). The number of times, when the URA size is optimal for the HT radar is shown in Fig. 9. Strangely enough, it is clearly seen that mostly there are two versions of the URA optimal

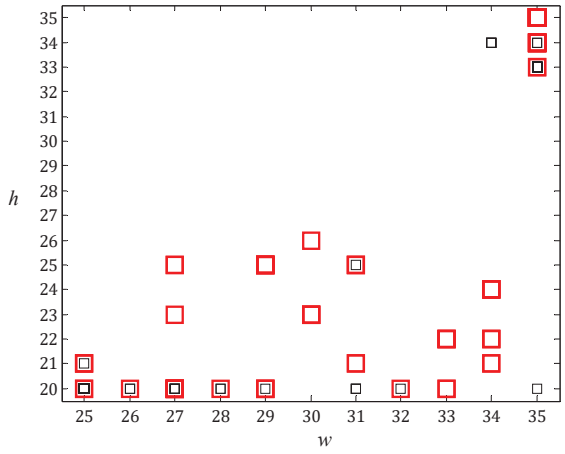

Fig. 8. The numbers of horizontal and vertical URA sensors optimal at the 499 detections

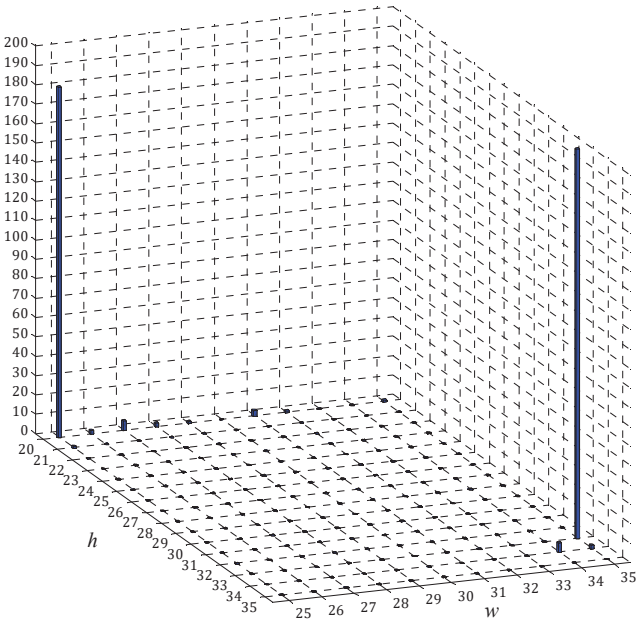

Fig. 9. Distribution of the URA optimal size for the 405 HT (and ST) radar detections

size: 20×25 and 33×35. The number of times, when the URA size is optimal for the 94 ST radar detections, when the HT radar detection failed, is shown in Fig. 10. The distribution here is more diverse, but the

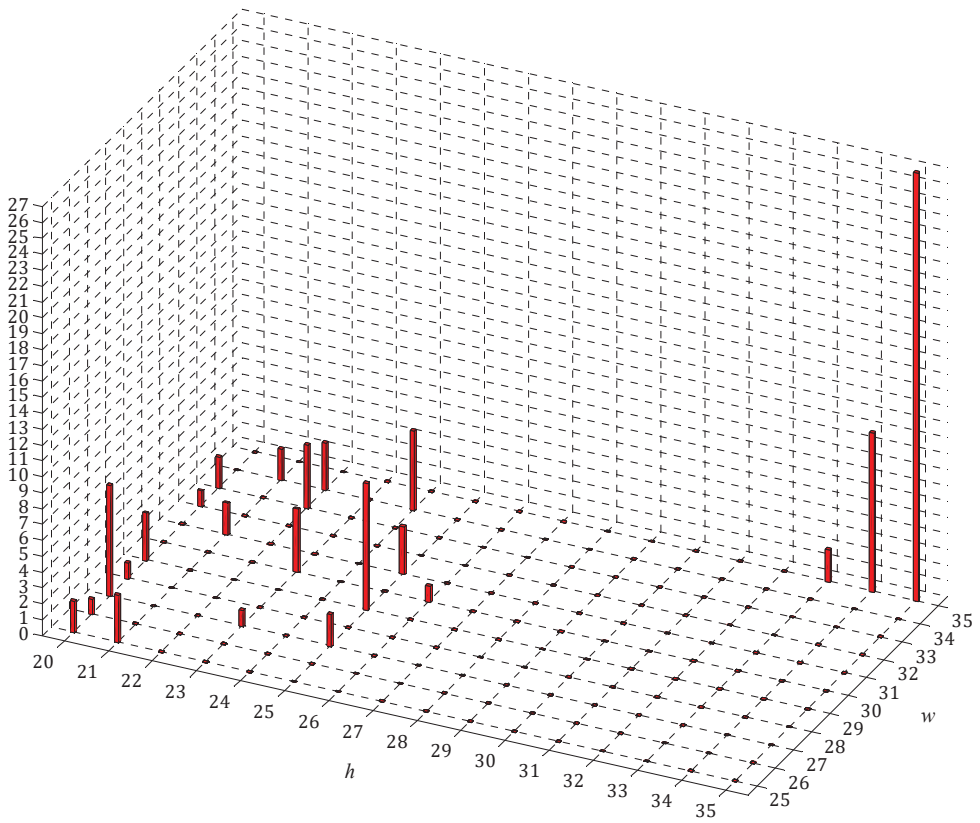

Fig. 10. Distribution of the URA size for the ST radar in the 94 cases, when the HT radar detection failed

optimal number of vertical sensors mostly is equal 20 to 25, although 34×35 and 35×35 URA radars have detected 10 and 27 targets, respectively. Therefore, the best decision on the URA size is to use, at the first stage, the minimally-sized URA (by turning off the maximal number of vertical and horizontal sensors). If the detection fails, then the maximally-sized URA radar is tried [36], [37]. If the detection fails again, the next minimally-sized URA is tried, in which one horizontal sensor is additionally turned on. Additional horizontal sensors should be turned on while the detection fails until the number of vertical sensors becomes greater by about a third of their minimal number. Thus, the radar can be successively tried with a set of URA sizes

$$20\times25,\ 35\times35,\ 20\times26,\ 34\times35,\ 20\times27,\ 33\times35,\ 20\times28,\ 34\times34,\ 20\times29,\ 33\times34,\ 20\times30,\ 33\times33$$

for 500 re-simulated targets (Fig. 11).

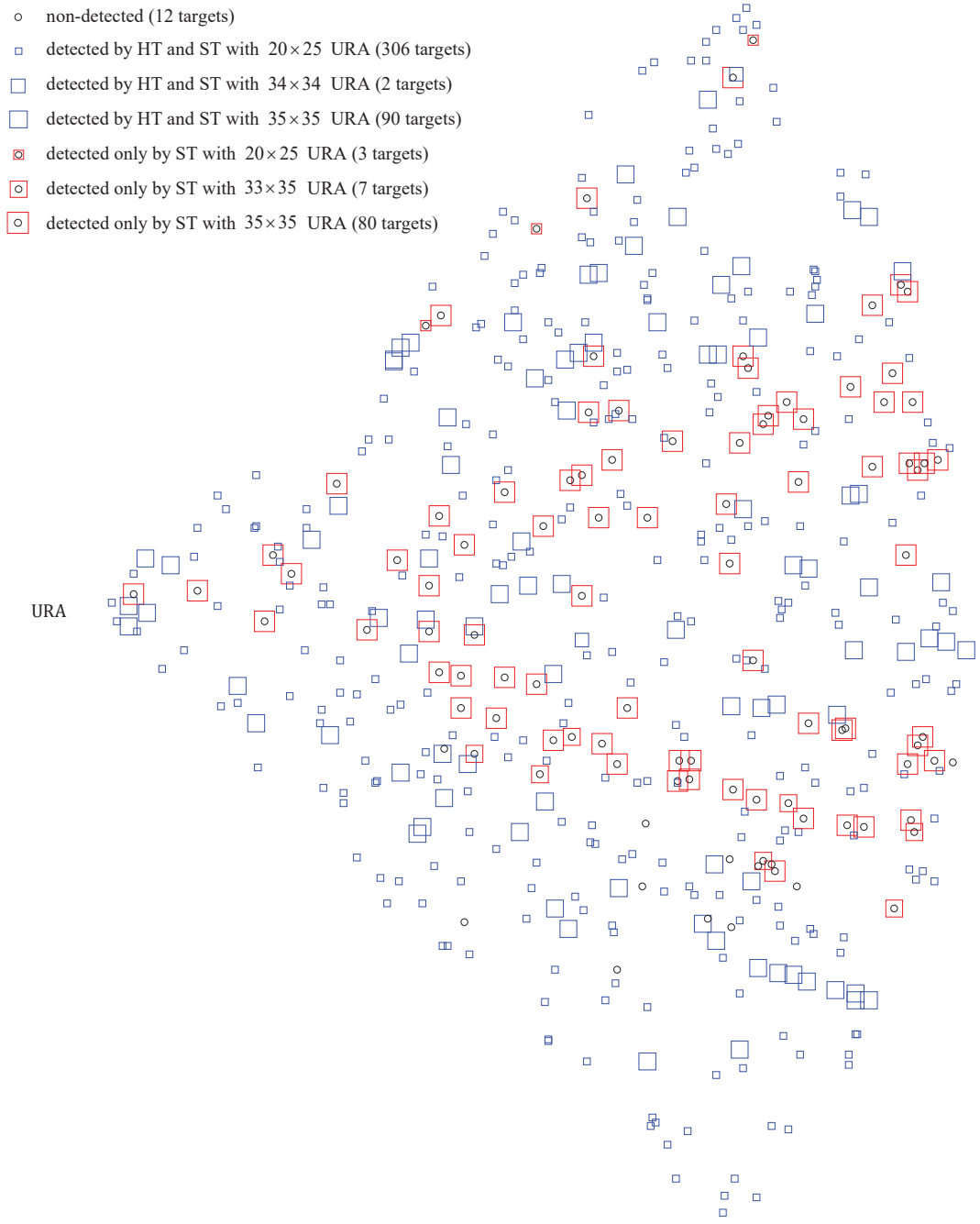

Fig. 11. The scatter of the 500 re-simulated targets, among which 398 targets have been detected by HT and ST radars, and 90 targets have been detected by only ST radar

5. Discussion

Clearly, Figs. 8 — 11 confirm that the suggested ST approach along with switching among quasioptimal URA sizes has a strong advantage. The URA radar is optimized in this way so that less targets are missed and the detection becomes slightly more accurate. However, the accuracy improvement is almost insignificant (see Table 1). This is the main limitation of the suggested optimization — the accurate estimation of target parameters means more targets are detected, where the parameters of every "additionally" detected target are estimated with approximately the same accuracy (on average) as it is for the non-optimized radar. In general, missing sufficiently less targets is a strong tradeoff.

One must remember that the detection accuracy cannot be estimated in real-world practice [6], [10], [18], [19], [38]. Thus, the statistics for the 94 detections by the detection threshold softer adjustment (see Table 2) is quite poor for unacceptable values of relative difference maximum (24). The case with (27) — (29) is a counterexample illustrating such "detections". This may be another tradeoff, for which some targets (whose number is small, though) are detected with huge inaccuracies of the estimated parameters (but a real-world observer, obviously, does not "suspect" that).

6. Conclusion

Based on simulating single-target detection, it is ascertained that an optimal number of URA radar sensors is in either the minimally-sized URA (or close to it) or maximally-sized URA (or close to it). The URA size is regulated by (symmetrically) turning off vertical and horizontal sensors. In addition, the threshold detection stage is modified so that the threshold is gradually decreased while the detection fails. This allows increasing a number of detected targets on average. It is equivalent to increasing the probability of detection at almost the same accuracy of estimated parameters of the target. The efficiency and accuracy of estimation is thus improved. The effect of the suggested optimization on detecting two targets simultaneously moving through the radar area is to be studied yet.

References

1. M. Skolnik, *Introduction to Radar Systems*, 3rd ed. New York City, New York, USA: McGraw-Hill, 2001.

2. L. Borowska, G. Zhang, and D. S. Zrnic, "Spectral processing for step scanning phased-array radars," *IEEE Transactions on Geoscience and Remote Sensing*, vol. 54, no. 8, pp. 4534 — 4543, 2016. https://doi.org/10.1109/TGRS.2016.2543724

3. R. Sturdivant, C. Quan, and E. Chang, *Systems Engineering of Phased Arrays*, Norwood, Massachusetts, USA: Artech House, 2018.

4. H. J. Visser, *Array and Phased Array Antenna Basics*, Hoboken, New Jersey, USA: John Wiley & Sons, 2006. https://doi.org/10.1002/0470871199

5. R. Gui, Z. Zheng, and W.-Q. Wang, "Cognitive FDA radar transmit power allocation for target tracking in spectrally dense scenario," *Signal Processing*, vol. 183, 108006, 2021. https://doi.org/10.1016/j.sigpro.2021.108006

6. P. Fritsche and B. Wagner, "Evaluation of a novel radar based scanning method," *Journal of Sensors*, vol. 2016, Article ID 6952075, 2016. https://doi.org/10.1155/2016/6952075

7. H. Asplund et al., "Chapter 4 — Antenna Arrays and Classical Beamforming," in *Advanced Antenna Systems for 5G Network Deployments: Bridging the Gap Between Theory and Practice*, P. von Butovitsch, Ed. Cambridge, Massachusetts, USA: Academic Press, 2020, pp. 89 — 132. https://doi.org/10.1016/B978-0-12-820046-9.00004-6

8. M.-M. Tamaddondar, H. Keshavarz, and J. Ahmadi-shokouh, "Beamsteering for non-uniform weighted array-fed reflector antenna," *Wireless Personal Communications*, vol. 97, pp. 5511 — 5525, 2017. https://doi.org/10.1007/s11277-017-4792-0

9. W. E. Kock, *Radar, Sonar, and Holography: An Introduction*, Cambridge, Massachusetts, USA: Academic Press, 1973. https://doi.org/10.1016/C2013-0-10981-6

10. R. J. Doviak and D. S. Zrnić, "Chapter 3 — Radar and Its Environment," in *Doppler Radar and Weather Observations*, 2nd ed. R. J. Doviak and D. S. Zrnić, Eds. Cambridge, Massachusetts, USA: Academic Press, 1993, pp. 30 — 63. https://doi.org/10.1016/B978-0-12-221422-6.50008-5

11. S. Alland, W. Stark, M. Ali, and M. Hegde, "Interference in automotive radar systems: characteristics, mitigation techniques, and current and future research," *IEEE Signal Processing Magazine*, vol. 36, no. 5, pp. 45 — 59, 2019. https://doi.org/10.1109/MSP.2019.2908214

12. W.-Q. Wang and H. Shao, "Radar-to-radar interference suppression for distributed radar sensor networks," *Remote Sensing*, vol. 6, iss. 1, pp. 740 — 755, 2014. https://doi.org/10.3390/rs6010740

13. G. Hakobyan, K. Armanious, and B. Yang, "Interference-aware cognitive radar: a remedy to the automotive interference problem," *IEEE Transactions on Aerospace and Electronic Systems*, vol. 56, no. 3, pp. 2326 — 2339, 2020. https://doi.org/10.1109/TAES.2019.2947973

14. W. Huang and R. Lin, "Efficient design of Doppler sensitive long discrete-phase periodic sequence sets for automotive radars," in *2020 IEEE 11th Sensor Array and Multichannel Signal Processing Workshop (SAM)*, Hangzhou, China, 2020, pp. 1 — 5. https://doi.org/10.1109/SAM48682.2020.9104358

15. C. Aydogdu et al., "Radar interference mitigation for automated driving: exploring proactive strategies," *IEEE Signal Processing Magazine*, vol. 37, no. 4, pp. 72 — 84, 2020.
https://doi.org/10.1109/MSP.2020.2969319
16. M. H. Er, "Array pattern synthesis with a controlled mean-square sidelobe level," *IEEE Transactions on Signal Processing*, vol. 40, no. 4, pp. 977 — 981, 1992. https://doi.org/10.1109/78.127971
17. F. Vincent, O. Besson, S. Abakar-Issakha, Laurent Ferro-Famil, and F. Bodereau, "On the tradeoff between resolution and ambiguities for non-uniform linear arrays," in *2016 IEEE Global Conference on Signal and Information Processing (GlobalSIP)*, Washington, USA, 2016, pp. 1052 — 1055.
18. L. Hongbo, S. Yiying, and L. Yongtan, "Estimation of detection threshold in multiple ship target situations with HF ground wave radar," *Journal of Systems Engineering and Electronics*, vol. 18, iss. 4, pp. 739 — 744, 2007.
https://doi.org/10.1016/S1004-4132(08)60013-4
19. H. Sun, M. Li, L. Zuo, and R. Cao, "Joint threshold optimization and power allocation of cognitive radar network for target tracking in clutter," *Signal Processing*, vol. 172, 107566, 2020.
https://doi.org/10.1016/j.sigpro.2020.107566
20. Z. Li and X. Zhang, "Monostatic MIMO radar with nested L-shaped array: Configuration design, DOF and DOA estimation," *Digital Signal Processing*, vol. 108, 102883, 2021.
https://doi.org/10.1016/j.dsp.2020.102883
21. A. Sleiman and A. Manikas, "The impact of sensor positioning on the array manifold," *IEEE Transactions on Antennas and Propagation*, vol. 51, no. 9, pp. 2227 — 2237, 2003.
https://doi.org/10.1109/TAP.2003.816333
22. N. Fourikis, "Chapter 2 — From Array Theory to Shared Aperture Arrays," in *Advanced Array Systems, Applications and RF Technologies: A volume in Signal Processing and its Applications*, N. Fourikis, Ed. Cambridge, Massachusetts, USA: Academic Press, 2020, pp. 111 — 217.
https://doi.org/10.1016/B978-012262942-6/50004-4
23. H. Gao, M. Chen, Y. Du, and A. Jakobsson, "Monostatic MIMO radar direction finding in impulse noise," *Digital Signal Processing*, vol. 117, 103198, 2021. https://doi.org/10.1016/j.dsp.2021.103198
24. M. K. Rad and S. M. H. Andargoli, "Power control and beamforming in passive phased array radars for low probability of interception," *Digital Signal Processing*, vol. 117, 103165, 2021.
https://doi.org/10.1016/j.dsp.2021.103165
25. Q. Cheng, S. Zheng, Q. Zhang, J. Ji, H. Yu, and X. Zhang, "An integrated optical beamforming network for two-dimensional phased array radar," *Optics Communications*, vol. 489, 126809, 2021.
https://doi.org/10.1016/j.optcom.2021.126809
26. I. Bahl and D. Hammers, "Chapter 4 — Phased-Array Radar," in *Gallium Arsenide IC Applications Handbook*, D. Fisher and I. Bahl, Eds. Cambridge, Massachusetts, USA: Academic Press, 1995, pp. 79 — 136.
https://doi.org/ 10.1016/B978-012257735-2/50005-X
27. D. W. O'Hagan, S. R. Doughty, and M. R. Inggs, "Chapter 5 — Multistatic radar systems," in *Academic Press Library in Signal Processing, Volume 7*, R. Chellappa and S. Theodoridis, Eds., Cambridge, Massachusetts, USA: Academic Press, 2018, pp. 253 — 275.
https://doi.org/10.1016/B978-0-12-811887-0.00005-5
28. D.-S. Jang, H.-L. Choi, and J.-E. Roh, "Search optimization for minimum load under detection performance constraints in multi-function phased array radars," *Aerospace Science and Technology*, vol. 40, pp. 86 — 95, 2015.
https://doi.org/10.1016/j.ast.2014.10.005
29. C. Wang, B. Jiu, and H. Liu, "Maneuvering target detection in random pulse repetition interval radar via resampling-keystone transform," *Signal Processing*, vol. 181, 107899, 2021.
https://doi.org/10.1016/j.sigpro.2020.107899
30. S. J. Orfanidis, *Electromagnetic Waves and Antennas*, Piscataway, New Jersey, USA: Rutgers University, 2016.
31. W. L. Stutzman and G. A. Thiele, *Antenna Theory and Design*, 3rd ed. Hoboken, New Jersey, USA: John Wiley & Sons, 2012.
32. H. Meikle, *Modern Radar Systems*, 2nd ed. Artech House Publishers, 2008.
33. T. A. Milligan, *Modern Antenna Design*, 2nd ed. Hoboken, New Jersey, USA: John Wiley & Sons, 2005.
https://doi.org/10.1002/0471720615
34. V. V. Romanuke, "Minimal total weighted tardiness in tight-tardy single machine preemptive idling-free scheduling," *Applied Computer Systems*, vol. 24, no. 2, pp. 150 — 160, 2019.
https://doi.org/10.2478/acss-2019-0019
35. V. V. Romanuke, "Decision making criteria hybridization for finding optimal decisions' subset regarding changes of the decision function," *Journal of Uncertain Systems*, vol. 12, no. 4, pp. 279 — 291, 2018.
36. V. V. Romanuke, "Interval uncertainty reduction via division-by-2 dichotomization based on expert estimations for short-termed observations," *Journal of Uncertain Systems*, vol. 12, no. 1, pp. 3 — 21, 2018.
37. V. V. Romanuke, "A minimax approach to mapping partial interval uncertainties into point estimates," *Journal of Mathematics and Applications*, vol. 42, pp. 147 — 185, 2019.
https://doi.org/10.7862/rf.2019.10
38. A. A. Mulla and P. N. Vasambekar, "Overview on the development and applications of antenna control systems," *Annual Reviews in Control*, vol. 41, pp. 47 — 57, 2016.
https://doi.org/10.1016/j.arcontrol.2016.04.012

Романюк В.В.

Оптимізація радара на основі рівномірно-прямокутної фазованої антенної решітки для ефективного та точного оцінювання параметрів об'єкта

Проблематика. Якщо інтенсивність рухомих об'єктів у межах спостережуваної області є низькою, деякі сенсори рівномірно-прямокутної фазованої антенної решітки (РПФАР) радара можуть бути (симетрично) вимкнуті. Однак це не гарантує виявлення будь-якого об'єкта, оскільки порогове виявлення, за яким оцінюються основні параметри об'єкта, не спрацьовує.

Мета дослідження. Для покращення виявлення наземних об'єктів необхідно знайти оптимальну кількість сенсорів РПФАР радара разом з удосконаленням етапу порогового виявлення. Критерієм є визначення такого мінімуму цих сенсорів, за якого основні параметри об'єкта оцінюються достатньо точно. Крім цього, порогове виявлення має бути змінене так, щоб кількість зривів виявлення була меншою.

Методика реалізації. Для досягнення мети проводиться симуляція РПФАР радара для виявлення одного об'єкта. Симуляція та її конфігурування відбуваються за допомогою функцій MATLAB® R2021b Phased Array System Toolbox™ на основі моделі моностатичного радара.

Результати дослідження. Існує множина квазіоптимальних розмірів РПФАР, до якої увійшли РПФАР мінімального та максимального розмірів. Найкращим рішенням є використати спершу РПФАР мінімального розміру (за допомогою вимкнення максимальної кількості вертикальних і горизонтальних сенсорів). Якщо виявлення не спрацьовує, то випробовується РПФАР максимального розміру. Якщо виявлення знову не спрацьовує, тоді випробовується наступна РПФАР мінімального розміру, у якій додатково вмикається один горизонтальний сенсор. Додаткові горизонтальні сенсори мають вмикатися доти, доки виявлення не спрацьовує, але кількість додаткових вертикальних сенсорів не має перевищити приблизно третини їх мінімальної кількості.

Висновки. Оптимальна кількість сенсорів РПФАР радара є або в РПФАР мінімального розміру (або близького до нього), або в РПФАР максимального розміру (або близького до нього). Розмір РПФАР регулюється за допомогою (симетричного) вимкнення вертикальних та горизонтальних сенсорів. Етап порогового виявлення модифікований так, що, поки виявлення не спрацьовує, поріг поступово зменшується. Це дозволяє збільшити кількість виявлених об'єктів у середньому, що еквівалентно підвищенню імовірності виявлення.

Ключові слова: *радар на основі фазованої антенної решітки; рівномірно-прямокутна антенна решітка; спостережувана область; об'єкт; поріг виявлення; точність.*